

Interaction between Neuronal Intranuclear Inclusions and Promyelocytic Leukemia Protein Nuclear and Coiled Bodies in CAG Repeat Diseases

Mitsunori Yamada,* Toshiya Sato,[†]
Takayoshi Shimohata,[†] Shintaro Hayashi,*
Shuichi Igarashi,[†] Shoji Tsuji,[†] and
Hitoshi Takahashi*

From the Departments of Pathology* and Neurology,[†] Brain
Research Institute, Niigata University, Niigata, Japan

Neuronal intranuclear inclusions (NIIs) are a pathological hallmark of CAG repeat diseases. To elucidate the influence of NII formation on intranuclear substructures, we investigated the relationship of NIIs with nuclear bodies in brains of dentatorubral-pallidoluysian atrophy and Machado-Joseph disease. In both diseases, promyelocytic leukemia protein, a major component of the promyelocytic leukemia protein nuclear bodies, altered the normal distribution and was rearranged around NII, forming a single capsular structure. We further demonstrated that NIIs were present in close contact with coiled bodies, a highly dynamic domain that may be involved in the biogenesis of small nuclear ribonucleoproteins. The preferential association of intranuclear polyglutamine aggregates with coiled bodies was also confirmed in the dentatorubral-pallidoluysian atrophy transgenic mouse brain and culture cells expressing mutant atrophin-1. The results suggest that the interaction between NIIs and nuclear bodies may play a role in the pathogenesis of CAG repeat diseases. (*Am J Pathol* 2001, 159:1785–1795)

It has been shown that the expansion of a CAG repeat encoding a polyglutamine (polyQ) tract is the causative mutation in at least eight neurodegenerative disorders, including Huntington's disease, dentatorubral-pallidoluysian atrophy (DRPLA), and Machado-Joseph disease (MJD).¹ Recently, with the exception of spinocerebellar ataxia type 6, the occurrence of neuronal intranuclear inclusions (NIIs) has been identified in the CAG repeat diseases,^{2–8} and in transgenic animal models.^{9–14} Because NIIs contain antigenicity of the causative gene products and expanded polyQ stretches, it is thought that these inclusions are a common hallmark of the polyQ diseases,¹ and may be closely related to the disease pathogenesis. The use of *in vitro* transient expression systems has revealed that the expression of truncated

proteins containing the expanded polyQ stretches results in the formation of aggregate bodies and causes cell apoptosis.^{5,7,8,15,16} The NII formation itself may be a cellular reaction to reduce the toxic effect of mutant proteins;^{17–19} however, an *in vitro* study²⁰ and our recent *in vitro* and *in vivo* studies^{21,22} have shown the recruitment of transcription factors such as TAF_{II}130 (TATA-binding protein-associated factor), CREB (cAMP-responsive element-binding protein), and CBP (CREB-binding protein) into an intranuclear aggregation of polyQ, suggesting that transcriptional abnormalities may be induced secondarily by NII formation, thus leading to cell death.

Another concern about the pathogenesis of CAG repeat diseases is the influence of NII formation on intranuclear structures. A recent *in vitro* study has indicated that large intranuclear aggregates, induced by mutant ataxin-1, sequester promyelocytic leukemia protein (PML) nuclear bodies and alter their normal nuclear distribution.⁸ The expression of mutant ataxin-3 in cultured cells also demonstrates the co-localization of intranuclear aggregates and PML nuclear bodies.²³ PML is a nuclear-matrix-associated protein and a component of PML nuclear bodies.^{24,25} A typical mammalian nucleus has 10 to 20 PML nuclear bodies, which vary in size from 0.3 to 1 μ m and are thought to be involved in growth regulation, transcriptional regulation, and apoptosis.^{24–26} Thus, the culture-based experiments suggest that in CAG repeat diseases, the alteration of intranuclear organizations may be induced by inclusion formation, which leads to nuclear dysfunction. To elucidate the effect of NII formation on intranuclear structures in human brains, in the present study we investigated the distribution of the PML nuclear body and the coiled body, the two most prominent subtypes of nuclear bodies.²⁷ We show that in both DRPLA and MJD brains, PML reorganizes a specific structure around NII with a unique distribution pattern that has not been observed in previous *in vitro* studies. In addition, this study is the first to report that NIIs may be found in

Supported by a grant from the Research Committee for Ataxic Diseases, the Ministry of Health, Labor, and Welfare, Japan; and a Grant-in-Aid for Scientific Research from the Ministry of Education, Culture, Sports, Science, and Technology, Japan.

Accepted for publication July 27, 2001.

Address reprint requests to Mitsunori Yamada, M.D., Department of Pathology, Brain Research Institute, Niigata University, 1 Asahimachi, Niigata 951-8585, Japan. E-mail: nori@bri.niigata-u.ac.jp.

contact with coiled bodies. The interaction between coiled bodies and intranuclear aggregates is also confirmed in the brains of DRPLA transgenic mice and an *in vitro* study. The present study clarifies the significant nuclear events involved in the formation of NIs, which may play a pivotal role in the pathological mechanisms of CAG repeat diseases in the human brain.

Materials and Methods

Human Materials and DRPLA Transgenic Mice

Brains obtained at autopsy from a patient with MJD (female, Q83, age 32 years), a patient with DRPLA (female, Q59, age 79 years), and seven controls (ages 65 to 83 years; mean, 73.4 years) served as the materials for the present study. We also examined the brains of transgenic mice harboring a single copy of a full-length human mutant DRPLA gene with 129 CAG repeats.²⁸ Because the occurrence of ubiquitinated NIs has been detected in mice after 9 weeks of age, for the present study we examined the cerebral cortex of mice at 14 weeks of age.

Immunohistochemistry

Tissue fragments of the pontine nuclei from each human brain were obtained at autopsy, quick-frozen in cold isopentane, and kept in a deep freezer until use. Cryostat sections (8- μ m thick) were made from the frozen materials, fixed with cold acetone (-20°C) for 7 minutes, and immunostained by the avidin-biotin-peroxidase complex (ABC) method with a Vectastain ABC kit (Vector Laboratories, Burlingame, CA), using either a rabbit antibody against ubiquitin (1:800), c-Jun (1:2000), c-Fos (1:2000), Egr-1 (1:2000), Egr-2 (1:2000), or Egr-3 (1:2000) as a primary antibody. Sections were incubated with the primary antibody for 18 hours at 4°C . Cryostat sections were also immunostained with either a mouse monoclonal antibody against PML (1:200) or SUMO-1 (1:200). With the exception of the anti-ubiquitin antiserum, which was purchased from Dakopatts (Glostrup, Denmark), the primary antibodies were purchased from Santa Cruz Biotechnology (Santa Cruz, CA). Diaminobenzidine was used as the chromogen. After immunostaining, the sections were counterstained with hematoxylin. To investigate the interaction of NIs with intranuclear structures, the cryostat sections were subjected to double-immunofluorescence staining. After incubation with 10% normal goat serum, sections were incubated with a mixture of a rabbit antibody against PML (1:50; Medical & Biological Laboratories, Nagoya, Japan) and a mouse monoclonal antibody against ubiquitin (1:50; Chemicon, Temecula, CA) for 18 hours at 4°C . For double-immunofluorescence staining of NIs and coiled bodies, a rabbit antibody against PML was replaced with a rabbit antibody against p80-coilin²⁹ (1:200; a gift from Dr. EK Chan, the Scripps Research Institute, La Jolla, CA). After washing with phosphate-buffered saline (PBS), the sections were incubated with a mixture of fluorescein-conjugated goat anti-mouse IgG (1:40; Cappel, Durham, NC) and rhodamine-conjugated

goat anti-rabbit IgG (1:40; Cappel) for 1 hour at room temperature, and observed with the aid of a fluorescence microscope. For negative controls, the primary antibody was replaced with normal rabbit or mouse serum. A brain was obtained from a DRPLA transgenic mouse (14 weeks of age), which had been sacrificed by overdose inhalation of ether. The cerebrum was cut coronally, and quick-frozen in cold isopentane. Cryostat sections were made from the frozen tissues and immunostained in the same manner as the human material.

COS-7 Cell Transfection and Immunocytochemistry

As described previously,⁵ COS-7 cells were transfected with a full-length or truncated DRPLA cDNA encoding 19 or 82 glutamine residues. At 48 hours after transfection, cells were fixed with 4% paraformaldehyde in 0.1 mol/L phosphate buffer (pH 7.4), permeabilized with 0.1% Triton X-100 in PBS, and then treated with 10% normal goat serum to quench nonspecific staining. Double-immunofluorescence staining was performed using a mixture of mouse anti-FLAG M5 monoclonal antibody (1:400; Eastman Kodak, Rochester, NY) and rabbit anti-PML antibody (1:200), or a mixture of mouse anti-FLAG M5 antibody (1:400) and rabbit anti-p80-coilin antibody (1:200) for 18 hours at 4°C , followed by incubation with secondary antibodies in the same manner as the double-immunofluorescence staining of the human brain sections described earlier.

Electron Microscopic Observation

For conventional electron microscopic examination, tissue fragments of the pontine nuclei were obtained at autopsy from a brain of a MJD patient, fixed in 3% glutaraldehyde-1% paraformaldehyde in 0.1 mol/L phosphate buffer, pH 7.4, postfixed in 1% osmium tetroxide, dehydrated through a graded ethanol series, and embedded in Epon 812 resin (Polysciences, Warrington, PA). A DRPLA transgenic mouse was deeply anesthetized by inhalation of ether, and then perfused transcardially with PBS followed by 3% glutaraldehyde-1% paraformaldehyde in 0.1 mol/L phosphate buffer, pH 7.4. After perfusion, the brain was removed from the cranium and immersed in the same fixative for a further 16 hours at 4°C . An age-matched nontransgenic mouse was prepared in the same way. The cerebral cortices of the mice were embedded in Epon 812 resin by the same method as the human brain tissue. Ultrathin sections were made from the tissue fragments, stained with uranyl acetate and lead citrate, and examined with a Hitachi-7100 electron microscope (Hitachi, Hitachinaka-city, Japan).

For immunoelectron microscopy, tissue fragments of the MJD pontine nuclei obtained at autopsy were fixed in 4% paraformaldehyde in 0.1 mol/L phosphate buffer, pH 7.4. A transgenic mouse was deeply anesthetized by inhalation of ether, and then perfused transcardially with the same fixative as was used to fix the human brain. The cerebral cortex was dissected out and prepared for anal-

ysis. The tissue fragments were dehydrated in a graded dimethylformamide series and embedded in LR White resin (London Resin Company, Berkshire, UK). Ultrathin sections were cut and mounted on nickel grids. After incubation with 10% normal goat serum for 10 minutes, the sections were incubated overnight at 4°C with a mixture of a rabbit antibody against PML (1:400) and a mouse monoclonal antibody against ubiquitin (1:50; Chemicon), or a mixture of a rabbit antibody against p80-coilin (1:200) and a mouse monoclonal antibody against ubiquitin (1:50; Chemicon). After washing with PBS, the sections were incubated with a mixture of a goat anti-rabbit IgG conjugated to 15-nm gold particles and a goat anti-mouse IgG conjugated to 10-nm gold particles (1:30; British BioCell International, Cardiff, UK) for 30 minutes at room temperature. The sections were then washed with PBS and incubated with 2% glutaraldehyde in 0.1 mol/L of sodium cacodylate buffer, pH 7.4. After washing with distilled water, the sections were stained with uranyl acetate and lead citrate, and examined with a Hitachi H-7100 electron microscope. For negative controls, the primary antibody was replaced with normal rabbit and mouse serum.

Results

Ubiquitinated NIIIs in the Brains of MJD and DRPLA Patients

To obtain the morphological details of NIIIs, we investigated the pontine nuclei of patients with MJD and DRPLA. In MJD, ubiquitinated NIIIs were observed in 54.4% of neurons. The number of NIIIs per nucleus varied, and the incidences of nuclei with a single, two (Figure 1a), three (Figure 1b), or more than three NIIIs was 25.3%, 73.4%, 0.6%, and 0.7%, respectively. In DRPLA, ubiquitinated NIIIs were observed in 8.5% of neurons, of which the number of nuclei with one, two, or three NIIIs was 67.6%, 30.9%, and 1.5%, respectively. The NIIIs varied in size from 0.8 to 3.7 μm in MJD, and from 0.7 to 2.2 μm in DRPLA. NIIIs were occasionally present in the vicinity of the nucleoli. In the case of neurons with two NIIIs per nucleus, the inclusions frequently appeared as pairs or doublets (70.3% in MJD and 71.5% in DRPLA, Figure 1a).

To assess the interaction of PML nuclear bodies with NIIIs in the human brain, we investigated immunohistochemically the localization of small ubiquitin-related modifier (SUMO-1), which is one of the constituent proteins of PML nuclear bodies.²⁴ In the normal brain, a diffuse distribution of SUMO-1 immunoreactivity was observed in the neuronal nucleoplasm (data not shown). In MJD and DRPLA brains, SUMO-1 immunoreactivity was co-localized with NIIIs and showed labeling patterns similar to that of ubiquitin immunohistochemistry, including the occurrence of paired shapes (Figure 1c). SUMO-1-immunoreactive NIIIs were observed in 56.3% and 2.8% of neurons in MJD and DRPLA, respectively. We examined further the interaction between transcription factors and NIIIs, and found that in both MJD and DRPLA, NIIIs were intensely immunopositive for c-Jun (Figure 1d) and weakly

immunopositive for c-Fos (data not shown), but were immunonegative for Egr-1, Egr-2, and Egr-3. In MJD and DRPLA, c-Jun-positive NIIIs were observed in 20.4% and 1.5% of neurons, respectively, and c-Fos-positive NIIIs were observed in 13.8% and 0.8% of neurons, respectively.

PML Nuclear Bodies in CAG Repeat Diseases, DRPLA Transgenic Mice, and Cultured Cells Transfected with DRPLA Protein with Expanded PolyQ Stretches

PML immunoreactivity appeared in normal neurons as 8 to 18 nuclear dots, which varied in size from 0.2 to 0.8 μm (Figure 1e). In MJD and DRPLA brains, PML labeling was rearranged in 47.1% and 11.0% of neurons, respectively, and formed a single large body (Figure 1f), which varied in size from 1.7 to 3.0 μm and from 1.5 to 2.3 μm , respectively. Most of these large PML structures were present solely in the neuronal nuclei; however, some bodies coexisted with a few PML dots of normal size. In neuronal nuclei that lacked the formation of large PML structures, there were no remarkable changes in their appearance and distribution. Double-immunofluorescence staining of MJD and DRPLA brains revealed that the large PML structures were co-localized with ubiquitinated NIIIs (Figure 1; g, h, and i). In the case of the single-type NIIIs, the incidence of the co-localization was as high as 94.4% in MJD and 83.9% in DRPLA. Interestingly, in the case of neurons harboring more than one NII per nucleus, the large PML structures were co-localized with only one of the NIIIs (Figure 1; j to l). In general, the PML-immunolabeling was larger than the ubiquitin-labeling, and was accentuated in the peripheral region of the NIIIs, exhibiting a donut-like appearance.

We examined the PML nuclear bodies of neurons in DRPLA transgenic mice carrying a single copy of a full-length human mutant DRPLA gene with 129 CAG repeats.²⁸ At 3 weeks of age these mice exhibited myoclonic movement. This was followed at up to 12 weeks of age by rapid progression of ataxia, myoclonic movement, and epilepsy; these animals all died by the age of 14 to 16 weeks. Neuropathologically, the brains showed progressive atrophy beginning as early as 4 weeks, but disclosed no apparent loss of neurons in any central nervous system (CNS) region until death. The occurrence of ubiquitinated NIIIs was first detectable at ~9 weeks of age in restricted regions of the CNS such as the subthalamic nucleus and the cerebellar nuclei. In the 14-week-old mouse brain, ubiquitinated NIIIs were present in a single form, and appeared in more extensive regions of the CNS including the cerebral cortex (layers II, III, IV, and VI), globus pallidus, thalamus, pontine nuclei, and the brainstem tegmentum, showing similarities with the pathology seen in human brains.³ In normal cerebral cortical neurons in 14-week-old mice, PML labeling appeared as multiple small dots in each nucleus, measuring from 0.3 to 0.6 μm in size, and scattered throughout the nucleoplasm. In the DRPLA transgenic mouse brain, cerebral cortical neurons lacking NIIIs showed no change in

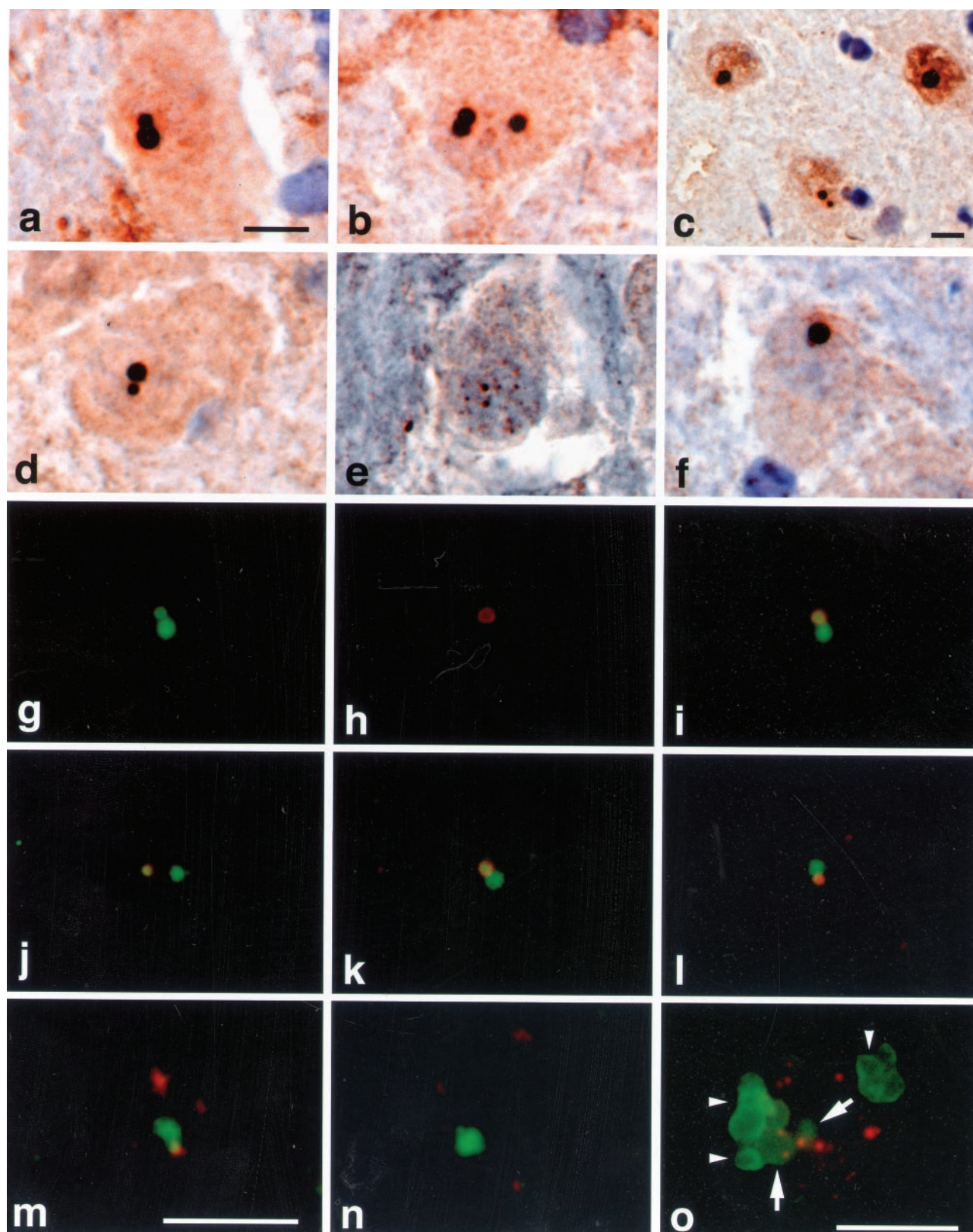


Figure 1. Immunohistochemistry for ubiquitin, small ubiquitin-related modifier (SUMO-1), c-Jun, and PML. These photographs (**a–l**) were taken from neurons in the pontine nuclei of a patient with MJD (**a–d, f–i**), a control case (**e**), and a patient with DRPLA (**j–l**). Ubiquitin labeling shows the presence of a doublet type of NII in a neuron harboring two (**a**) or three (**b**) NIIs. SUMO-1 is co-localized on NIIs with weak labeling in the nucleoplasm (**c**). NIIs are intensely immunopositive for c-Jun (**d**). PML labeling in neuronal nuclei appears as small intranuclear dots in control tissue (**e**), but as a large body in MJD (**f**). Double-immunofluorescence staining with anti-ubiquitin (green color) and anti-PML (red color) antibodies reveals a neuron that contains a doublet type of ubiquitinated NIIs (**g**), and large donut-shaped PML labeling (**h**) is co-localized on one of the paired NIIs (shown by yellow color in **i**) with a larger labeled area around the NII. The restricted co-localization of PML labeling on one NII is seen in other neurons of MJD (**j** and **k**) and DRPLA (**l**) brains. In the cerebral cortical

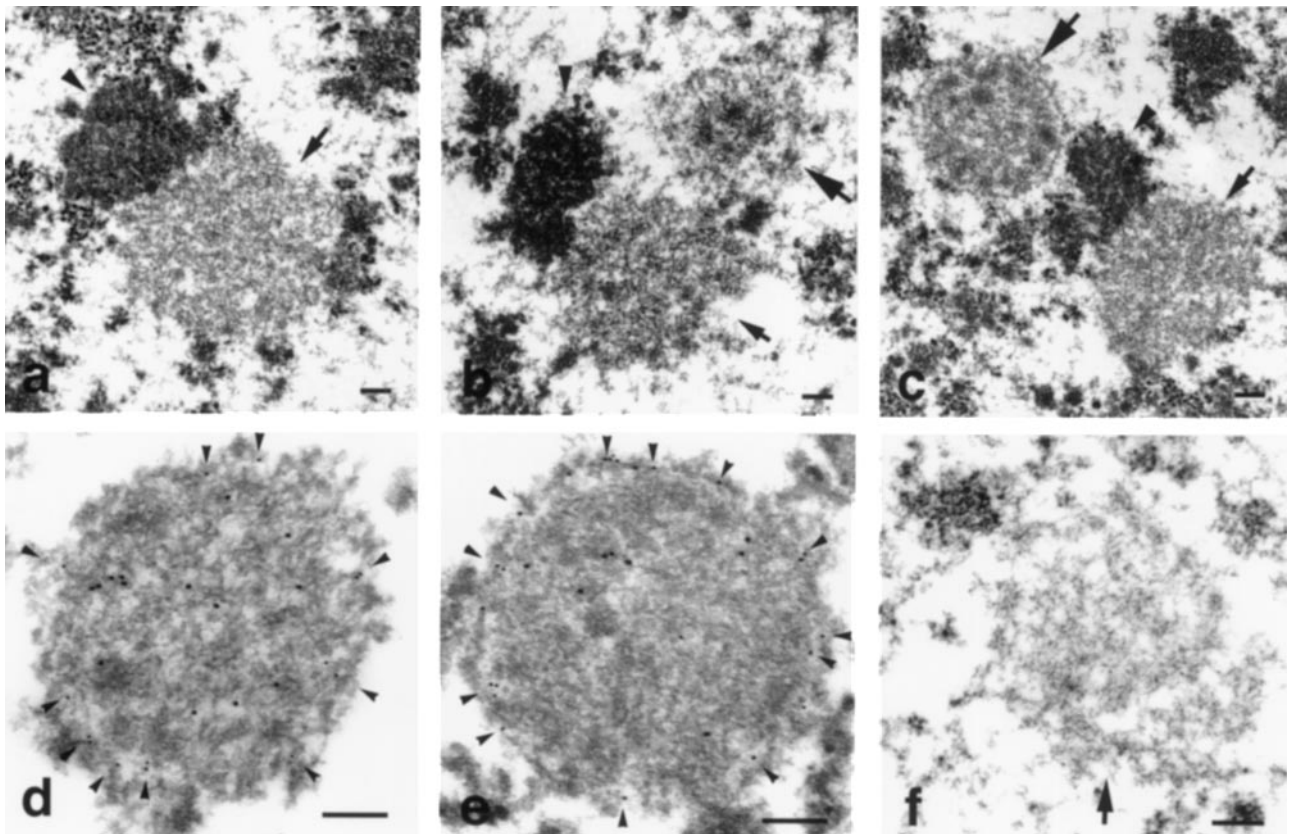


Figure 2. Ultrastructure of NIIs in the pontine nuclei of a MJD brain (**a–e**) and in the cerebral cortex of a DRPLA transgenic mouse (**f**). With the aid of a conventional electron microscope (**a–c**), it appears that NIIs (**arrows**) are composed of a mixture of granular and filamentous structures. Large **arrows** in **b** and **c** indicate NIIs with ring-like structures around their fibrillar cores. Neurons harboring two NIIs (**b** and **c**) show that a ring-like structure is formed around only one of the two NIIs. Granulofibrillar bodies (**arrowheads** in **a–c**), which are morphologically identical to coiled bodies, are present in contact with NIIs. Double-immunogold-labeling (**d** and **e**) for ubiquitin (indicated by 15-nm gold particles) and PML (indicated by 10-nm gold particles) shows that PML is localized in the marginal zone of NIIs (**arrowheads** in **d**) or on the ring-like structure around the NIIs (**arrowheads** in **e**). No PML labeling is seen on a NII (**arrow**) of a DRPLA transgenic mouse (**f**). Scale bars, 200 nm.

the PML-labeling pattern. Most of the cortical neurons harboring NIIs also retained the scattered pattern of PML labeling (Figure 1, m and n), but the association of a few PML dots was occasionally encountered around some NIIs (Figure 1m). The large donut-like labeling of PML seen in human brains was not observed in these young mouse brains.

We examined the distribution of PML nuclear bodies in COS-7 cells expressing mutant DRPLA protein. As observed in our previous study,⁵ the formation of aggregate bodies was restricted to cells expressing truncated DRPLA protein with 82 glutamines, and observed mostly in the perinuclear regions of the cytoplasm, and less frequently in the nuclei. In cells lacking aggregate formation, PML nuclear bodies appeared as multiple intranuclear dots 0.3 to 1.1 μm in size, and were scattered throughout the nucleoplasm. In cells harboring intranuclear aggregates, PML nuclear bodies retained their mul-

tipple dot-like appearance, but some were recruited around the aggregates (Figure 1o). Cells with only cytoplasmic aggregates showed no apparent changes in the distribution of PML nuclear bodies. The immunohistochemical studies using human and mouse brains, as well as cultured cells, revealed no positive staining in the control tissue.

Localization of PML to the Ring-Like Structure Surrounding NIIs

To elucidate the precise localization of PML, we conducted an ultrastructural analysis of the NIIs of a MJD patient. Conventional electron microscopic examination revealed that NIIs lacked a limiting membrane, were heterogeneous in composition, and contained a mixture of granular and filamentous structures (Figure 2a). The fila-

Figure 1 continued.

neurons of a DRPLA transgenic mouse harboring a full-length human mutant DRPLA gene with 129 CAG repeats (**m** and **n**), a few small PML-immunopositive dots are observed associated with NIIs. In a COS-7 cell that was cultured for 48 hours after transfection with a truncated DRPLA cDNA encoding 82 glutamine residues (**o**), intranuclear aggregates (**arrows**) are observed associated with some PML-immunopositive dots within the nucleus (red color). Intracytoplasmic (**arrowheads**) and intranuclear (**arrows**) aggregates are shown as a green color, using anti-FLAG M5 antibody. Immunoperoxidase (**a–f**) and double-immunofluorescence (**g–o**) methods. Scale bars, 10 μm . The scale bar in photograph **a** also applies to photographs **b** and **d** to **m**, and the scale bar in photograph **m** also applies to photograph **n**.

mentous composition was straight or slightly curved, ~12 to 15 nm in diameter, and usually organized in random, but sometimes parallel arrays. Although we did not observe neuronal nuclei with more than two inclusions per nucleus, nuclei with two NILs were occasionally encountered when viewed with the aid of an electron microscope. These twin-type NILs were also composed of granular and filamentous structures similar to those of the single-type NILs. Occasionally, NILs were surrounded by ring-like structures, which were basically composed of granular materials and exhibited various appearances from broad circles with an irregular and vague contour, to a clear-ring architecture (Figure 2, b and c). Interestingly, in the case of the nuclei harboring two inclusions per nucleus, the formation of ring-like structures was restricted to only one of the NILs (Figure 2, b and c). Electron microscopic immunohistochemistry using immunogold labeling revealed that PML immunoreactivity was present in both types of NILs, those lacking or harboring the ring-like structures. In the case of the former type, labeling was scattered rather broadly at the marginal region of the NILs (Figure 2d). In the case of the latter, however, PML labeling was more concentrated on the ring architecture (Figure 2e). Ubiquitin immunoreactivity was essentially present on the core structure of the NILs, and was rarely observed intermingled with PML labeling, even in NILs lacking a ring-like structure (Figure 2d).

We also examined ultrastructurally the NILs of DRPLA transgenic mice. Examination of semithin sections of cerebral cortical layers II and III of these mice showed that NILs were formed in 50.8% of neurons, and neurons harboring NILs had many indentations in the nuclear membrane. Cerebral cortical neurons of a nontransgenic mouse brain exhibited mostly smooth-surfaced, round nuclei that lacked any inclusions. Ultrastructural examination showed that NILs in DRPLA transgenic mice were solitary, nonmembrane-bound, and varied in size from 1.2 to 2.2 μm . NILs were relatively homogeneous in composition and composed mainly of fibrous structures, which were fundamentally straight, ~9 to 12 nm in diameter, and organized in random arrays. The ring-like structures seen around the NILs of the MJD brain were not observed in DRPLA transgenic mice. No labeling for PML protein was detected on or around NILs (Figure 2f), as revealed using immunoelectron microscopy.

Close Association of NILs with p80-Coilin-Immunopositive Structures

To clarify the interaction of NILs with intranuclear structures, we investigated further, immunohistochemically, the localization of p80-coilin, a constituent protein of coiled bodies,³⁰ in MJD and DRPLA brains. In the neuronal nuclei of normal human brains, p80-coilin immunoreactivity appeared as dots measuring up to 1.7 μm . Most neurons showed the presence of a single coiled body in a nucleus (Figure 3a), but some had a few or more smaller coiled bodies per nucleus (Figure 3b). In the MJD brain, no apparent changes were observed in

the distribution and sizes of p80-coilin labeling; however, some neuronal nuclei showed paired immunolabeling (Figure 3c) similar to that observed with ubiquitin immunohistochemistry. Double-immunofluorescence studies revealed that most of the ubiquitinated NILs were distinct from structures positive for p80-coilin, but both were present in close contact with each other (Figure 3; d to g). This relationship was also confirmed in the DRPLA human brain (Figure 3, h and i). In the case of the single-type NILs, the incidence of the adjoining of NILs and coiled bodies was 76.7% in MJD and 83.3% in DRPLA. The rest of the single-type NILs mostly lacked p80-coilin labeling in any nuclear regions of the examined section. When observed with the aid of fluorescence microscopy, most of the paired NILs were associated with one or more coiled bodies (Figure 3, f and g). In some nuclei, p80-coilin lost its normal dot-like distribution, and was co-localized with ubiquitinated NILs (Figure 3; j, k, and l). Contacts or partial co-localization of NILs with p80-coilin labeling were also observed in the cerebral cortical neurons of DRPLA transgenic mice (Figure 3, m and n), with the incidence reaching as high as 93.1% of NILs. Labeling for p80-coilin appeared as a few dots (~1.1 μm) in most of neuronal nuclei, and there were no apparent changes between normal and transgenic mice in the size and distribution of the labeled structures. In COS-7 cells, p80-coilin-labeling appeared as a few discrete round dots measuring from 0.4 to 1.0 μm . Although there were no apparent differences in the size and distribution of coiled bodies between cells harboring or lacking the aggregates of mutant protein, intranuclear aggregates were frequently associated with p80-coilin-positive structures (Figure 3o).

Association of NILs with Coiled Bodies

To elucidate the morphology of p80-coilin-immunopositive dots in neuronal nuclei, we subjected NILs in the MJD brain to immunoelectron microscopic observation. Immunogold labeling for p80-coilin was localized on granulo-fibrillar structures (Figure 4; a, b, and c) that were round to oval in shape, measured from 0.5 to 1.0 μm in diameter, and corresponded morphologically to the coiled body.^{31,32} These labeled structures were present in contact with NILs (Figure 4a), and were occasionally positioned between two NILs (Figure 4, b and c). The association of NILs with coiled bodies was observed frequently, even when viewed using conventional electron microscopy (Figure 2; a, b, and c, arrowheads).

We investigated further the relationship between NILs and coiled bodies in the cerebral cortical neurons of DRPLA transgenic mice. The association between granulo-fibrillar bodies and NILs was encountered frequently when viewed with the aid of an electron microscope (Figure 4d), and the incidence reached as high as 77.8% of NIL sections ($n = 126$). The morphology of the granulo-fibrillar bodies was consistent with that of coiled bodies, and the size varied, probably because of the level at which the bodies were sectioned, reaching up to 0.9 μm in diameter. The bodies possessed radially oriented fila-

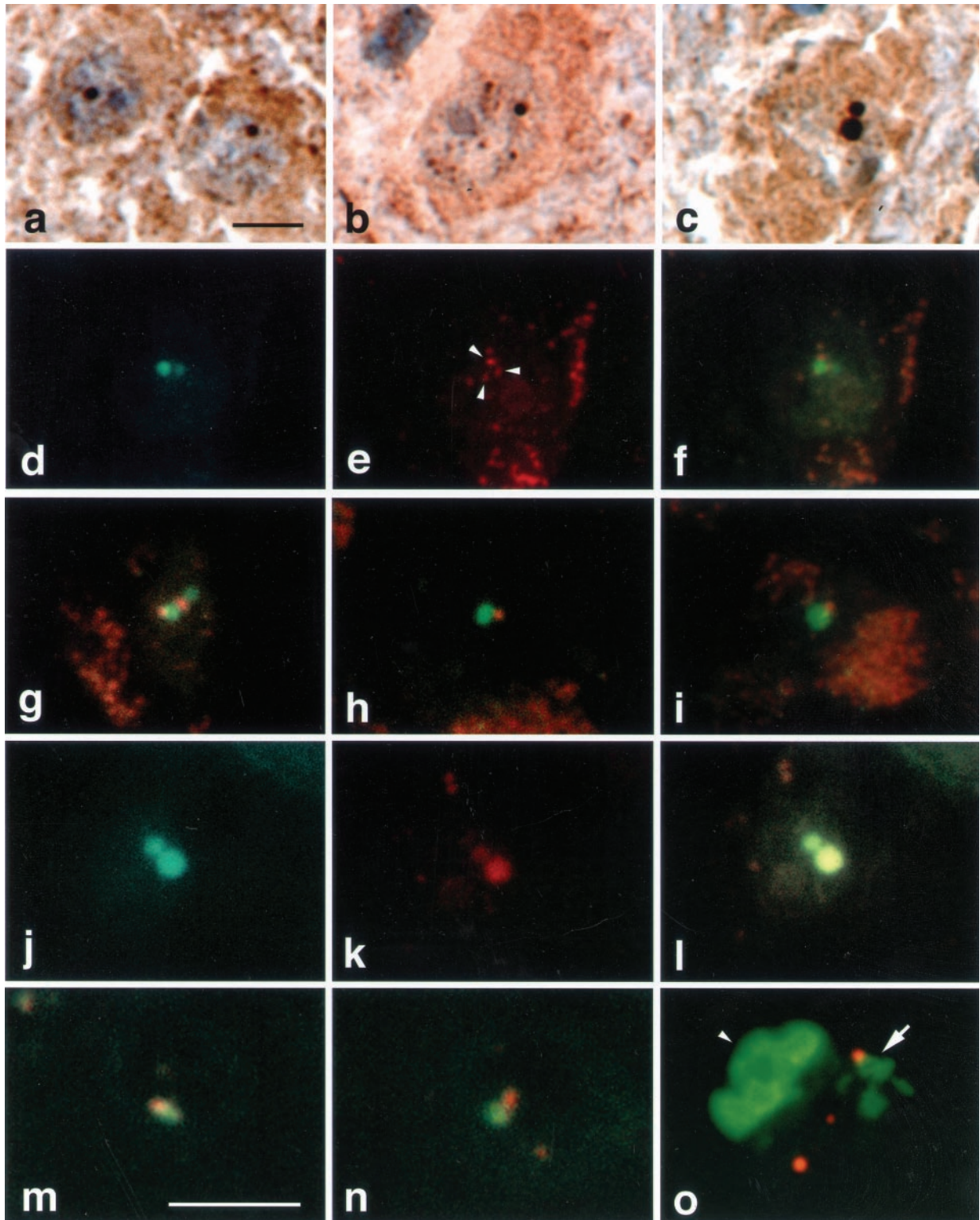


Figure 3. Immunohistochemistry for ubiquitin and p80-coilin, a specific marker of coiled bodies. These photographs (a–l) were taken from neurons in the pontine nuclei of MJD (a–g, j–l) and DRPLA (h and i) brains. Coilin labeling appears in neuronal nuclei as small round bodies of various sizes (a and b), and rarely shows NII-like appearance as larger bodies (c). Double-immunofluorescence staining with anti-ubiquitin and anti-p80-coilin antibodies reveals that ubiquitinated NIIs (green color in d) and coiled bodies (red color in e, indicated by **arrowheads**) are present in a nucleus in association with each other (f). The association between NIIs and coiled bodies is seen in other neurons of MJD (g) and DRPLA (h and i) brains. A rare case of co-localization of p80-coilin on NIIs is shown in photographs j (NIIs), k (p80-coilin), and l (shown in a yellow color by merged image). The association between NIIs and coiled bodies is also seen in the cerebral cortical neurons of a DRPLA transgenic mouse (m and n). In a COS-7 cell transfected with a truncated DRPLA cDNA encoding 82 glutamine residues (o), a group of intranuclear aggregates (**arrow**) is present in contact with a coiled body. Aggregates occur within the nucleus and the cytoplasm (**arrowhead**) and are shown in a green color, using anti-FLAG M5 antibody. The granular labeling observed in the cytoplasm (e–i) is autofluorescence by lipofuscin granule. Immunoperoxidase (a–c) and double-immunofluorescence (d–o) methods. Scale bars, 10 μ m. The scale bar in photograph a also applies to photographs b to l, and the scale bar in photograph m also applies to photographs n and o.

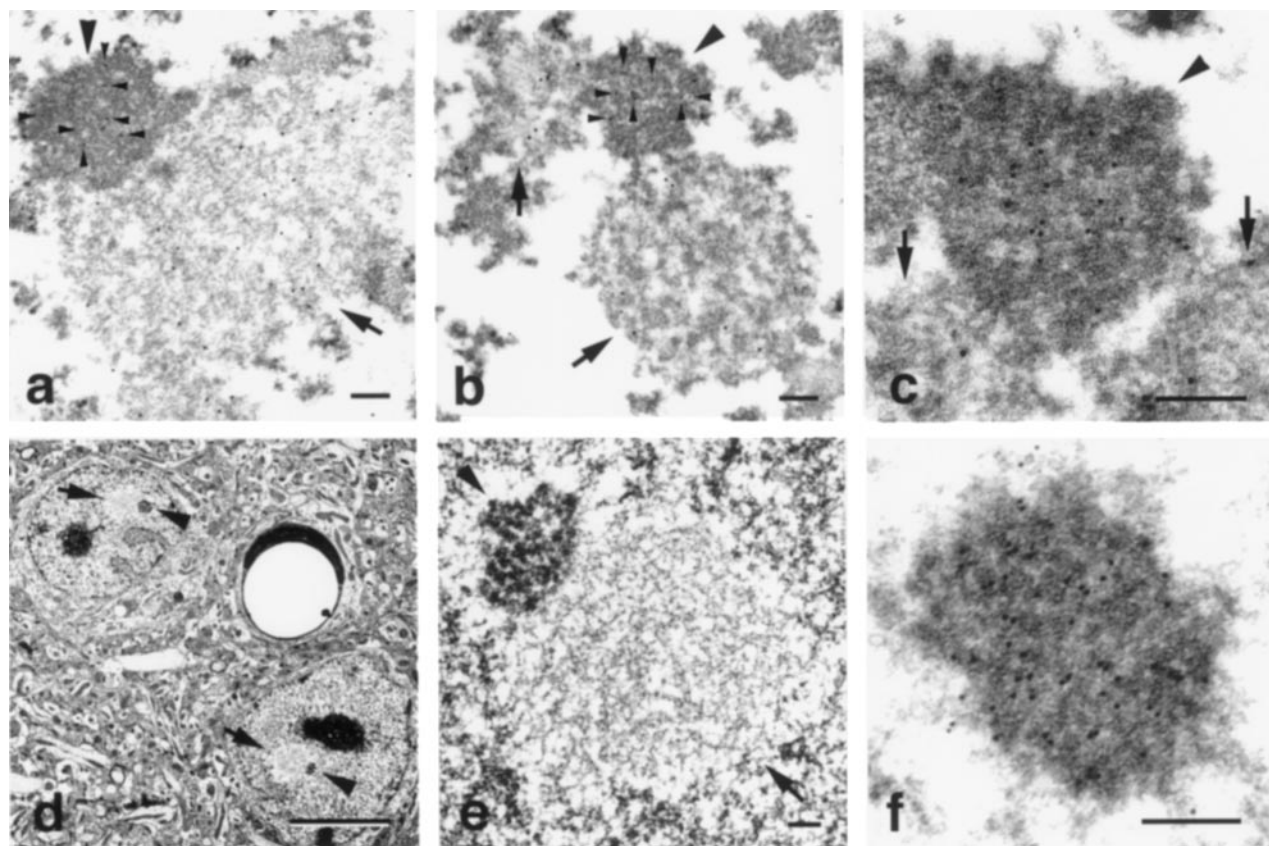


Figure 4. Ultrastructure of NIIs in the pontine nuclei of a MJD brain (**a–c**) and in the cerebral cortex of a DRPLA transgenic mouse (**d–f**). Double-immunogold labeling (**a–c**) for ubiquitin (indicated by 15-nm gold particles) and p80-coilin (indicated by 10-nm gold particles, **small arrowheads**) shows that the p80-coilin-labeled structure is the coiled body (**large arrowhead**), which is present in contact with one or two NIIs (**arrows**). Two cerebral cortical neurons in a DRPLA transgenic mouse show the presence of a single NII (**arrows**) that is associated with an electron-dense body (**arrowheads**). Photograph **e** shows that the electron-dense body (**arrowhead**) is a granulofibrillar body that is morphologically identical to the coiled body, and a NII (**arrow**) that is connected to the coiled body by filamentous structures. The immunogold method indicates that the granulofibrillar body is positive for p80-coilin, as indicated by the 10-nm gold particles (**f**). Scale bars, 200 nm.

ments around the granulofibrillar core, and NIIs were connected with these filamentous structures (Figure 4e). Electron microscopic immunohistochemistry confirmed the granulofibrillar cores to be positive for p80-coilin (Figure 4f). In the neuronal nuclei of nontransgenic mouse brains, the granulofibrillar bodies were encountered in 11.1% of nucleus sections. No apparent differences were observed in the size and appearance of granulofibrillar bodies, including the surrounding filaments, between the transgenic and nontransgenic mice.

Discussion

The results of the present study indicate that at least two subnuclear structures are commonly but distinctly involved in NII formation in both DRPLA and MJD. The immunohistochemical analyses showed that in neuronal nuclei harboring NIIs, PML proteins altered their normal distribution and were rearranged around NIIs, giving them a donut-like appearance. This rearrangement is in accordance with the results of *in vitro* studies in which the expression of mutant ataxin-1⁸ or ataxin-3²³ was investigated. In these studies, PML nuclear bodies were observed to have been recruited on the large intranuclear

aggregates of mutant proteins. It is possible that this structural change causes certain nuclear dysfunctions that result in cell death. The present immunoelectron microscope study, however, disclosed that the antigenicity of PML protein is localized on fibrillar ring-like structures around NIIs. In the case of NIIs lacking the fibrillar ring, PML labeling was distributed in a circular manner, at the periphery of NIIs. In typical PML nuclear bodies of normal cells, PML protein is specific for a dense fibrillar ring surrounding a central core, or for a filamentous component at the margin of nuclear bodies.^{33,34} Thus, we think that the donut-like labeling of PML around NIIs does not represent merely aggregates of PML nuclear bodies, but rather may be a specific structure that has been actively reorganized by PML in retaining the original nature of PML distribution. In contrast to human brains, the donut-like PML rearrangement was not observed in DRPLA transgenic mice or culture experiments. Considering the short period of time after the formation of the aggregates in the mouse brain and cultured cells, PML remodeling may be time consuming. Recent studies have indicated that PML nuclear bodies are involved in the proteasome-mediated degradation of ubiquitinated proteins.³⁵ It has also been reported that PML contains a

RING-finger domain,³⁵ which can act as a ubiquitin-protein ligase (E3) targeting proteins for degradation.^{36,37} Thus, the concentration of PML around NIIIs may suggest that PML is actively participating in the degradation of NIIIs through the physiological ubiquitin-proteasome pathway, rather than being recruited by NIIIs.

It is interesting that in the present study PML was concentrated on one NII per nucleus, even when more than one ubiquitinated NII was present in a nucleus. This predilection was not observed in previous culture experiments forming multiple intranuclear aggregates of mutant proteins.^{8,23} As disclosed by the ultrastructural study, NIIIs were heterogeneous in composition. Therefore, a certain specific type of NII may be present in each nucleus, which in turn may be related to the predilection of PML for a particular NII, although we were unable to describe the morphological features common to the NIIIs that were associated with PML. Alternatively, the concentration of PML may depend on the order of NII formation. From our results, we speculate that most of the PMLs are concentrated in the first NII that is formed in a nucleus. In other words, the formation of the first NII within a nucleus might exert a certain influence on the subsequent distribution of PML and bring about the accumulation of the protein to itself, even when another NII has been formed. At present, it remains to be demonstrated whether in human brain pathology more than one NII is formed simultaneously in a nucleus from the beginning. However, we have shown that in DRPLA transgenic mice single NII formation is an essential event in the brain during at least the period from ~9 weeks (an initial stage of NII formation) up to 16 weeks (maximal survival time of the mice) of age.

In contrast to PML, SUMO-1 was distributed prevalently among NIIIs. SUMO-1 is a protein with a ubiquitin-homology domain, and it covalently modifies specific nuclear proteins such as PML and Sp100, another PML nuclear body-associated protein.³⁸ This modification by SUMO-1 (sumoylation) has been proposed to play a role in directing the proteins to specific subnuclear compartments such as PML nuclear bodies, rather than targeting them to proteasomal degradation.³⁹ This implicates a role for SUMO-1 in the compartmentalization of certain proteins into NIIIs. Alternatively, SUMO-1 may function in protecting specific proteins from degradation at NIIIs. As indicated in recent studies,^{21,22,40,41} several transcription factors such as CBP and p53 are recruited into intranuclear inclusions. The present study also demonstrated the co-localization of c-Jun and c-Fos in NIIIs. The fact that p53 and c-Jun are targets of ubiquitin and are also substrates for SUMO-1 that enable it to avoid ubiquitination,⁴² may suggest that SUMO-1 plays a role in protein stability in NIIIs. It is likely, however, that the recruitment of many kinds of nuclear proteins into NIIIs leads to gradual nuclear dysfunction, eventually resulting in neuronal atrophy or degeneration.

Another striking feature revealed by the present study is the close association between NIIIs with coiled bodies. This association was observed in DRPLA and MJD brains, DRPLA transgenic mouse brains, and cultured cells, forming intranuclear aggregates with mutant DR-

PLA protein. The common occurrence of this phenomenon among different diseases suggests that the contact is dependent on the expanded polyQ stretches within the causative DRPLA protein or ataxin-3. Ultrastructurally, NIIIs and coiled bodies were observed either in direct contact with each other or connected to each other by filamentous structures (Figure 4e). The molecular basis of this interaction is a matter of interest; however, it is unlikely that p80-coilin mediates this connection, because the molecule does not contain any clearly recognizable peptide motifs⁴³⁻⁴⁵ or polyQ domains, the latter of which have the potential to interact with mutant extended polyQ.²⁰ Electron microscopic immunohistochemistry for p80-coilin also failed to label either the connecting filaments or the NIIIs. Between proteins contained in coiled bodies,^{27,46} TATA-binding protein may be one of the candidates involved in the connection, because TATA-binding protein contains a particularly long polyQ stretch and is recruited in the NIIIs of DRPLA and MJD brains.²¹

The function of coiled bodies is not fully understood. They contain small nuclear ribonucleoprotein particles, which are involved in splicing, and recent studies have suggested that these structures play a role in small nuclear ribonucleoprotein particle biogenesis.^{25,27} The coiled body is a highly dynamic structure that undergoes assembly and disassembly during the cell cycle, the number of changes being related to cell growth and gene expression level.^{25,47} Although in the present study the coiled bodies showed no apparent changes in their morphology and distribution, it is possible that their close interaction with NIIIs may result indirectly in alterations in the function of coiled bodies. It is feasible that because of their relatively large size, NIIIs interfere with the motility of coiled bodies.⁴⁸ This interference may extend to the intimate relationship between the coiled body and the nucleoli.^{25,27} To elucidate the mechanisms that underlie neuronal cell death in CAG repeat diseases, it is now necessary to explore how the association between NIIIs and coiled bodies affects the function of the latter. Aside from the influence of NIIIs, the preferential association between NIIIs and coiled bodies may explain the reason why NIIIs are frequently present in paired or doublet form when more than one NII is present in a nucleus. As revealed by electron microscopy, coiled bodies were frequently observed sandwiched between two NIIIs.

Acknowledgments

We thank S. Egawa, Y. Ohta, T. Hasegawa, C. Tanda, J. Takasaki, and K. Honma for their technical assistance; M. Machida, K. Abe, and T. Koike for their secretarial assistance; and E. K. Chan for generously providing the anti-p80-coilin antiserum.

References

1. Ross CA: Intranuclear neuronal inclusions: a common pathogenic mechanism for glutamine-repeat neurodegenerative diseases? *Neuron* 1997, 19:1147-1150

2. DiFiglia M, Sapp E, Chase KO, Davies SW, Bates GP, Von-sattel JP, Aronin N: Aggregation of huntingtin in neuronal intranuclear inclusions and dystrophic neurites in brain. *Science* 1997, 277:1990–1993
3. Hayashi Y, Kakita A, Yamada M, Koide R, Igarashi S, Takano H, Ikeuchi T, Wakabayashi K, Egawa S, Tsuji S, Takahashi H: Hereditary dentatorubral-pallidoluysian atrophy: detection of widespread ubiquitinated neuronal and glial intranuclear inclusions in the brain. *Acta Neuropathol* 1998, 96:547–552
4. Holmberg M, Duyckaerts C, Dürr A, Cancel G, Gourfinkel-An I, Damié P, Faucheux B, Trotter Y, Hirsch EC, Agid Y, Brice A: Spinocerebellar ataxia type 7 (SCA7): a neurodegenerative disorder with neuronal intranuclear inclusions. *Hum Mol Genet* 1998, 7:913–918
5. Igarashi S, Koide R, Shimohata T, Yamada M, Hayashi Y, Takano H, Date H, Oyake M, Sato T, Egawa S, Ikeuchi T, Tanaka H, Nakano R, Tanaka K, Hozumi I, Inuzuka T, Takahashi H, Tsuji S: Suppression of aggregate formation and apoptosis by transglutaminase inhibitions in cells expressing truncated DRPLA protein with an expanded polyglutamine stretch. *Nat Genet* 1998, 18:111–117
6. Koyano S, Uchihara T, Fujigasaki H, Nakamura A, Yagishita S, Iwabuchi K: Neuronal intranuclear inclusions in spinocerebellar ataxia type 2: triple-labeling immunofluorescent study. *Neurosci Lett* 1999, 273:117–120
7. Paulson HL, Perez MK, Trotter Y, Trojanowski JQ, Subramony SH, Das SS, Vig P, Mandel J-L, Fischbeck KH, Pittman RN: Intranuclear inclusions of expanded polyglutamine protein in spinocerebellar ataxia type 3. *Neuron* 1997, 19:333–344
8. Skinner PJ, Koshy BT, Cummings CJ, Klement IA, Helin K, Servadio A, Zoghbi HY, Orr HT: Ataxin-1 with an expanded glutamine tract alters nuclear matrix-associated structures. *Nature* 1997, 389:971–974
9. Davies SW, Turmaine M, Cozens BA, DiFiglia M, Sharp AH, Ross CA, Scherzinger E, Wanker EE, Mangiarini L, Bates GP: Formation of intranuclear inclusions underlies the neurological dysfunction in mice transgenic for the HD mutation. *Cell* 1997, 90:537–548
10. Mangiarini L, Sathasivam K, Seller M, Cozens B, Harper A, Hetherington C, Lawton M, Trotter Y, Leach H, Davies SW, Bates GP: Exon 1 of the HD gene with an expanded CAG repeat is sufficient to cause a progressive neurological phenotype in transgenic mice. *Cell* 1996, 87:493–506
11. Ross CA, Wood JD, Schilling G, Peters MF, Nucifora Jr FC, Cooper JK, Sharp AH, Margolis RL, Borchelt DR: Polyglutamine pathogenesis. *Phil Trans R Soc Lond B* 1999, 354:1005–1011
12. Schilling G, Becher MW, Sharp AH, Jinnah HA, Duan K, Kotzka JA, Slunt HH, Ratovitski T, Cooper JK, Jenkins NA, Copeland NG, Price DL, Ross CA, Borchelt DR: Intranuclear inclusions and neuritic aggregates in transgenic mice expressing a mutant N-terminal fragment of huntingtin. *Hum Mol Genet* 1999, 8:397–407
13. Schilling G, Wood JD, Duan K, Slunt HH, Gonzales V, Yamada M, Cooper JK, Margolis RL, Jenkins NA, Copeland NG, Takahashi H, Tsuji S, Price DL, Borchelt DR, Ross CA: Nuclear accumulation of truncated atrophin-1 fragments in a transgenic mouse model of DRPLA. *Neuron* 1999, 24:275–286
14. Warrick JM, Paulson HL, Gray-Board GL, Bui QT, Fischbeck KH, Pittman RN, Bonini NM: Expanded polyglutamine protein forms nuclear inclusions and causes neural degeneration in *Drosophila*. *Cell* 1998, 93:939–949
15. Ikeda H, Yamaguchi M, Sugai S, Aze Y, Narumiya S, Kakizuka A: Expanded polyglutamine in the Machado-Joseph disease protein induces cell death in vitro and in vivo. *Nat Genet* 1996, 13:196–202
16. Martindale D, Hackam A, Wiczorek A, Ellerby L, Wellington C, McCutcheon K, Singaraja R, Kazemi-Esfarjani P, Devon R, Kim SU, Bredesen DE, Tufaro F, Hayden MR: Length of huntingtin and its polyglutamine tract influences localization and frequency of intracellular aggregates. *Nat Genet* 1998, 18:150–154
17. Cummings CJ, Reinstein E, Sun Y, Antalffy B, Jiang Y, Ciechanover A, Orr HT, Beaudet AL, Zoghbi HY: Mutation of the E6-AP ubiquitin ligase reduces nuclear inclusion frequency while accelerating polyglutamine-induced pathology in SCA1 mice. *Neuron* 1999, 24:879–892
18. Klement IA, Skinner PJ, Kaytor MD, Yi H, Hersch SM, Clark HB, Zoghbi HY, Orr HT: Ataxin-1 nuclear localization and aggregation: role in polyglutamine-induced disease in SCA1 transgenic mice. *Cell* 1998, 95:41–53
19. Saudou F, Finkbeiner S, Devys D, Greenberg ME: Huntingtin acts in the nucleus to induce apoptosis but death does not correlate with the formation of intranuclear inclusions. *Cell* 1998, 95:55–66
20. Kazantsev A, Preisinger E, Dranovsky A, Goldgaber D, Housman D: Insoluble detergent-resistant aggregates form between pathological and nonpathological lengths of polyglutamine in mammalian cells. *Proc Natl Acad Sci USA* 1999, 96:11404–11409
21. Shimohata T, Nakajima T, Yamada M, Uchida C, Onodera O, Naruse S, Kimura T, Koide R, Nizaki K, Sano Y, Ishiguro H, Sakoe K, Ooshima T, Sato A, Ikeuchi T, Oyake M, Sato T, Aoyagi Y, Hozumi I, Nagatsu T, Takiyama Y, Nishizawa M, Goto J, Kanazawa I, Davidson I, Tanese N, Takahashi H, Tsuji S: Expanded polyglutamine stretches interact with TAF₁₃₀: interfering with CREB-dependent transcription. *Nat Genet* 2000, 26:29–36
22. Nucifora Jr FC, Sasaki M, Peters MF, Huang H, Cooper JK, Yamada M, Takahashi H, Tsuji S, Troncoso J, Dawson VL, Dawson TM, Ross CA: Interference by huntingtin and atrophin-1 with CBP-mediated transcription leading to cellular toxicity. *Science* 2001, 23:2423–2428
23. Chai Y, Koppenhafer SL, Shoesmith SJ, Perez MK, Paulson HL: Evidence for proteasome involvement in polyglutamine disease: localization to nuclear inclusions in SCA3/MJD and suppression of polyglutamine aggregation in vitro. *Hum Mol Genet* 1999, 8:673–682
24. Hodges M, Tissot C, Howe K, Grimwade D, Freemont PS: Structure, organization, and dynamics of promyelocytic leukemia protein nuclear bodies. *Am J Hum Genet* 1998, 63:297–304
25. Lamond AI, Earnshaw WC: Structure and function in the nucleus. *Science* 1998, 280:547–553
26. Seeler JS, Dejean A: The PML nuclear bodies: actors or extras? *Curr Opin Genet Dev* 1999, 9:362–367
27. Matera AG: Nuclear bodies: multifaceted subdomains of the interchromatin space. *Trends Cell Biol* 1999, 9:302–309
28. Sato T, Yamada M, Oyake M, Nakao K, Nakamura M, Katsuki H, Takahashi H, Tsuji S: Transgenic mice harboring a full-length human DRPLA gene with highly expanded CAG repeats exhibit severe disease phenotype. *Am J Hum Genet* 1999, 65(Suppl):A30
29. Andrade LE, Tan EM, Chan EK: Immunocytochemical analysis of the coiled body in the cell cycle and during cell proliferation. *Proc Natl Acad Sci USA* 1993, 90:1947–1951
30. Raska I, Andrade LE, Ochs RL, Chan EK, Chang CM, Roos G, Tan EM: Immunological and ultrastructural studies of the nuclear coiled body with autoimmune antibodies. *Exp Cell Res* 1991, 195:27–37
31. Monneron A, Bernhard W: Fine structural organization of the interphase nucleus in some mammalian cells. *J Ultrastruct Res* 1969, 27:266–288
32. Lafarga M, Hervas JP, Santa-Cruz MC, Villegas J, Crespo D: The "accessory body" of Cajal in the neuronal nucleus. A light and electron microscopic approach. *Anat Embryol* 1983, 166:19–30
33. Koken GH, Puvion-Dutilleul F, Guillemin MC, Viron A, Linares-Cruz G, Stuurman N, de Jong L, Szosteki C, Calvo F, Chomienne C, Degos L, Puvion E, de Thé H: The t(15;17) translocation alters a nuclear body in a retinoic acid-reversible fashion. *EMBO J* 1994, 13:1073–1083
34. Sternsdorf T, Grotzinger T, Jensen K, Will H: Nuclear dots: actors on many stages. *Immunobiology* 1997, 198:307–331
35. Reyes JC: PML and COP1—two proteins with much in common. *Trends Cell Biol* 2001, 26:18–20
36. Joazeiro CA, Wing SS, Huang H, Levenson JD, Hunter T, Liu YC: The tyrosine kinase negative regulator c-Cbl as a RING-type, E2-dependent ubiquitin-protein ligase. *Science* 1999, 286:309–312
37. Lorick KL, Jensen JP, Fang S, Ong AM, Hatakeyama S, Weissman AM: RING fingers mediate ubiquitin-conjugating enzyme (E2)-dependent ubiquitination. *Proc Natl Acad Sci USA* 1999, 96:11364–11369
38. Sternsdorf T, Jensen K, Will H: Evidence for covalent modification of the nuclear dot-associated proteins PML and Sp100 by PIC1/SUMO-1. *J Cell Biol* 1997, 139:1621–1634
39. Müller S, Matunis MJ, Dejean A: Conjugation with the ubiquitin-related modifier SUMO-1 regulates the partitioning of PML within the nucleus. *EMBO J* 1998, 17:61–70
40. Steffan JS, Kazantsev A, Spasic-Boskovic O, Greenwald M, Zhu YZ, Gohler H, Wanker EE, Bates GP, Housman DE, Thompson LM: The Huntington's disease protein interacts with p53 and CREB-binding protein and represses transcription. *Proc Natl Acad Sci USA* 2000, 97:6763–6768
41. McCampbell A, Taylor JP, Taye AA, Robitschek J, Li M, Walcott J,

- Merry D, Chai Y, Paulson H, Sobue G, Fischbeck KH: CREB-binding protein sequestration by expanded polyglutamine. *Hum Mol Genet* 2000, 9:2197–2202
42. Müller S, Berger M, Lehenbre F, Seeler JS, Haupt Y, Dejean A: c-Jun and p53 activity is modulated by SUMO-1 modification. *J Biol Chem* 2000, 275:13321–13329
43. Bauer DW, Murphy C, Wu Z, Wu CH, Gall JG: In vitro assembly of coiled bodies in *Xenopus* egg extract. *Mol Biol Cell* 1994, 5:633–644
44. Bohmann K, Ferreira JA, Lamond AI: Mutational analysis of p80 coilin indicates a functional interaction between coiled bodies and the nucleolus. *J Cell Biol* 1995, 131:817–831
45. Chan EK, Takano S, Andrade LE, Hamel JC, Matera AG: Structure, expression and chromosomal localization of human p80-coilin gene. *Nucleic Acids Res* 1994, 22:4462–4469
46. Schul W, van Driel R, de Jong L: Coiled bodies and U2 snRNA genes adjacent to coiled bodies are enriched in factors required for snRNA transcription. *Mol Biol Cell* 1998, 9:1025–1036
47. Lamond AI, Carmo-Fonseca M: The coiled body. *Trends Cell Biol* 1993, 3:198–204
48. Platini M, Goldberg I, Swedlow JR, Lamond AI: In vivo analysis of Cajal body movement, separation, and joining in live human cells. *J Cell Biol* 2000, 151:1561–1574